Long, low loss etched As_2S_3 chalcogenide waveguides for all-optical signal regeneration

S. J. Madden[1*], D-Y. Choi[1], D. A. Bulla[1], A. V. Rode[1], B. Luther-Davies[1], V.G. Ta'eed[2], M.D. Pelusi[2] and B.J. Eggleton[2]

[1]Centre for Ultrahigh-Bandwidth Devices & Optical Systems (CUDOS)
Laser Physics Centre, Research School of Physical Science and Engineering, Australian National University, Canberra, ACT 0200, Australia
[2]Centre for Ultrahigh-Bandwidth Devices & Optical Systems (CUDOS)
School of Physics, University of Sydney, NSW 2006, Australia
[*]Corresponding Author: sjm111@rsphysse.anu.edu.au

http://www.cudos.org.au

Abstract: We report on the fabrication and optical properties of etched highly nonlinear As_2S_3 chalcogenide planar rib waveguides with lengths up to 22.5 cm and optical losses as low as 0.05 dB/cm at 1550 nm - the lowest ever reported. We demonstrate strong spectral broadening of 1.2 ps pulses, in good agreement with simulations, and find that the ratio of nonlinearity and dispersion linearizes the pulse chirp, reducing the spectral oscillations caused by self-phase modulation alone. When combined with a spectrally offset band-pass filter, this gives rise to a nonlinear transfer function suitable for all-optical regeneration of high data rate signals.

OCIS codes: (060.4510) Optical communications; (070.4340) Nonlinear optical signal processing; (130.3120) Integrated optics devices

References and links

1. J. T. Gopinath, M. Soljacic, E. P. Ippen, V. N. Fuflyigin, W. A. King, and M. Shurgalin, "Third order nonlinearities in Ge-As-Se-based glasses for telecommunications applications," J. Appl. Phys. **96**, 6931-6933 (2004).
2. R. G. DeCorby, N. Ponnampalam, M. M. Pai, H. T. Nguyen, P. K. Dwivedi, T. J. Clement, C. J. Haugen, J. N. McMullin, and S. O. Kasap, "High index contrast waveguides in chalcogenide glass and polymer," IEEE J. Sel. Top. Quantum Electron. **11**, 539-546 (2005).
3. S. Ramachandran, and S. G. Bishop, "Photoinduced integrated-optic devices in rapid thermally annealed chalcogenide glasses," IEEE J. Sel. Top. Quantum Electron. **11**, 260-270 (2005).
4. Y. L. Ruan, B. Luther-Davies, W. T. Li, A. Rode, V. Kolev, and S. Madden, "Large phase shifts in AS_2S_3 waveguides for all-optical processing devices," Opt. Lett. **30**, 2605-2607 (2005).
5. A. V. Rode, A. Zakery, M. Samoc, R. B. Charters, E. G. Gamaly, and B. Luther-Davies, "Laser-deposited As_2S_3 chalcogenide films for waveguide applications," Appl. Surf. Sci. **197**, 481-485 (2002).
6. A. K. Mairaj, P. Hua, H. N. Rutt, and D. W. Hewak, "Fabrication and characterization of continuous wave direct UV (λ=244 nm) written channel waveguides in chalcogenide (Ga : La : S) glass," J. Lightwave Technol. **20**, 1578-1584 (2002).
7. N. Ponnampalam, P. Dwivedi, T. Allen, T. Clement, R. DeCorby, and Y Tsui, Conference on Laser Ablation COLA'05, Banf, Canada, 11-16 September 2005.
8. Y. A. Vlasov, and S. J. McNab, "Losses in single-mode silicon-on-insulator strip waveguides and bends," Opt. Express **12**, 1622-1631 (2004).
9. N. Ho, J. M. Laniel, R. Vallee, and A. Villeneuve, "Photosensitivity of As_2S_3 chalcogenide thin films at 1.5 μm," Opt. Lett. **28**, 965-967 (2003).
10. K. K. Lee, D. R. Lim, H. C. Luan, A. Agarwal, J. Foresi, and L. C. Kimerling, "Effect of size and roughness on light transmission in a Si/SiO_2 waveguide: Experiments and model," Appl. Phys. Lett. **77**, 1617-1619 (2000).
11. P. V. Mamyshev, "All-optical data regeneration based on self-phase modulation effect," in Proceedings of European Conference on Optical Communication (ECOC)(Madrid, Spain, 1998), pp. 475-476.

#87277 - $15.00 USD Received 7 Sep 2007; revised 14 Oct 2007; accepted 15 Oct 2007; published 18 Oct 2007

12. W. T. Li, Y. L. Ruan, B. Luther-Davies, A. Rode, and R. Boswell, "Dry-etch of As_2S_3 thin films for optical waveguide fabrication," J. Vac. Sci. Technol. A **23**, 1626-1632 (2005).
13. D. G. Georgiev, P. Boolchand, and K. A. Jackson, "Intrinsic nanoscale phase separation of bulk As_2S_3 glass," Philosophical Magazine **83**, 2941-2953 (2003).
14. H. Takeuchi, and K. Oe, "Low-Loss Single-Mode Gaas Algaas Miniature Optical Wave-Guides with Straight and Bending Structures," J. Lightwave Technol. **7**, 1044-1054 (1989).
15. see e.g. D. L. Wood, and J. Tauc, "Weak Absorption Tails in Amorphous Semiconductors," Phys. Rev. B **5**, 3144-& (1972).
16. A. Zakery, Y. Ruan, A. V. Rode, M. Samoc, and B. Luther-Davies, "Low-loss waveguides in ultrafast laser-deposited As2S3 chalcogenide films", J. Opt. Soc. Am. B, **20**, 1844-1852 (2003).
17. M. Lamont, C.M. de Sterke, and B. Eggleton, "Dispersion engineering of highly nonlinear As_2S_3 waveguides for parametric gain and wavelength conversion," Opt. Express **15**, 9458-9463 (2007).
18. V. G. Ta'eed, M. Shokooh-Saremi, L. B. Fu, D. J. Moss, M. Rochette, I. C. M. Littler, B. J. Eggleton, Y. L. Ruan, and B. Luther-Davies, "Integrated all-optical pulse regenerator in chalcogenide waveguides," Opt. Lett. **30**, 2900-2902 (2005).
19. G. P. Agrawal, Nonlinear Fiber Optics (Academic Press, San Diego, 2001).
20. L. B. Fu, M. Rochette, V. G. Ta'eed, D. J. Moss, and B. J. Eggleton, "Investigation of self-phase modulation based optical regeneration in single mode As_2Se_3 chalcogenide glass fiber," Opt. Express **13**, 7637-7644 (2005).

1. Introduction

Chalcogenide glasses are promising candidates for planar non-linear optical (NLO) waveguide devices due to their large NLO coefficients, high refractive index, and low linear and non-linear optical losses [e.g. 1]. A surge in planar activity over the last 10 years has seen a diverse range of fabrication techniques yield reasonably low loss planar waveguides in the As_2S_3, As_2Se_3, As-S-Se, Ga-La-S, Ge-As-Se and Ge-As-S-Se systems, amongst others, with losses down to 0.2dB/cm at 1550nm at best in any system [2-7].

However, to attain sub-Watt thresholds for all-optical processing of high data rate (160Gb/s) telecommunications signals in chalcogenide glass waveguides, advances are required that lead to a simultaneous reduction in the mode area of the waveguide and an increase in waveguide length. In chalcogenide glasses it is not practical to simply follow the route used, for example, with silicon nanowire waveguides of shrinking to very small sizes [8]. Firstly, chalcogenide glass films have damage mechanisms that limit the short term maximum fluence in the waveguide to $\approx$1 GW/cm^2 [9]. Secondly their ultra-fast Kerr response leads to relatively small index changes (10^{-5} to 10^{-4}) compared with materials such as silicon, whose index change is resonantly enhanced by the generation of free carriers. Hence device lengths of several tens of centimeters are mandatory.

At present the usable length of chalcogenide planar waveguides is loss-limited, and reduction of the mode area is challenging since waveguide loss often increases as the waveguide cross-section decreases due to scattering induced by surface roughness [10]. These problems can be overcome using improved process technology as well as waveguide designs that suppress field enhancement at the etched sidewall surfaces as the waveguide is shrunk to smaller dimensions.

In this paper we report significant advances on both of these aspects of NLO waveguides resulting in As_2S_3 chalcogenide planar rib waveguides with lengths up to 22.5 cm and optical losses as low as 0.05 dB/cm at 1550 nm. We demonstrate strong nonlinear spectral broadening of 1.2 ps optical pulses in excellent agreement with simulations by the split-step Fourier method. The simulations show that the chromatic dispersion of these waveguides enhances their performance when used for self-phase modulation based signal regeneration [11].

2. Planar waveguide fabrication

As_2S_3 films were deposited from commercially available glass (Amorphous Materials, Garland, Texas, USA) using thermal evaporation from a Tungsten boat in a chamber pumped to a base pressure of 3×10^{-7} Torr. The boat temperature during evaporations was controlled at

#87277 - $15.00 USD Received 7 Sep 2007; revised 14 Oct 2007; accepted 15 Oct 2007; published 18 Oct 2007

315˚C giving a deposition rate of 0.1-0.3 nm/s for a source to substrate distance of ≈40 cm. Films were deposited on <100> oriented 100 mm silicon wafers with 1.5 µm of thermal oxide. The wafers were placed in a carousel rotated with planetary motion leading to a thickness uniformity of ±0.02 µm for a 2.6 µm thick film. Depositions were made to obtain films either 2.6 µm or 0.9 µm thick. The refractive index of the as deposited films was 2.29 at 1550 nm as determined from wafer mapping with a 450-1650 nm dual angle spectroscopic reflectometer (SCI Filmtek 4000). Note that the large deviation from the bulk glass index (2.43 at 1550 nm) is a characteristic of chalcogenide glass films that arises from variations in the bond structure between the film and bulk material. Observation of the films using dark field microscopy revealed a smooth surface with a small number (~1/cm^2) of droplet-like particles. The wafers were annealed in vacuum at 130˚C for 24 hours, after which the refractive index had risen to 2.37 at 1550 nm. Waveguide ribs were patterned using standard contact photolithography. Nominal waveguide widths were 4 µm and the mask incorporated two serpentine "snake" patterns as well as straight waveguides. The "snakes" were comprised of 3 straight sections of waveguide connected with two 180˚ circular arc bends as shown in Fig. 1.

Fig. 1. "Snake" pattern layout schematic, inner bend radius was 2.5mm, outer radius was 3.2mm

The two snake patterns were 17 and 24 cm long measured to the wafer edge. Special attention was paid to mask fabrication, the photo-mask having a measured line edge roughness on straight waveguides of 6 nm RMS for a spatial fluctuation wavelength range of 0.6 to 62 µm. Around the bends, the optical mask writer discretization could not be totally suppressed, leading to higher RMS roughness of ~20 nm for the 1.85 cm of total bend length. Lateral confinement trenches were etched 0.9 µm or 0.4 µm deep in the 2.6 µm and 0.9 µm films respectively in an inductively coupled plasma reactive ion etcher with CHF_3 gas. Previously, a CF_4 and O_2 gas mix had been employed to etch waveguides [12]. A characteristic of this etch chemistry was differential etching of the different phases present in the As_2S_3 films which are known to be inherently phase-separated [13]. This led to an increase in the surface roughness after etching. As this is clearly an undesirable effect, considerable effort was invested to develop an etch process which provided smoother surfaces. Experimentation revealed that the main cause of surface roughening was the high proportion of reactive Fluorine present in a $CF_4 + O_2$ plasma which led to enhanced chemical etching of some phases of the material. The use of CHF_3 reduces the concentration of Fluorine radicals and additionally provides some sidewall and surface passivation via the deposition of fluorocarbon polymers, which is well known to enhance etch anisotropy. Optimization of the etch conditions produced a process that also gave excellent dimensional control and close to vertical sidewalls.

The final plasma conditions were 25 sccm CHF_3, 2 sccm O_2, 5 mT process pressure, 40 W substrate bias power, 400 W ICP power (Oxford Instruments 100 series ICP etcher). The etched surface roughness was better than halved compared to the $CF_4 + O_2$ process as shown in Fig. 2 from AFM scans.

#87277 - $15.00 USD Received 7 Sep 2007; revised 14 Oct 2007; accepted 15 Oct 2007; published 18 Oct 2007

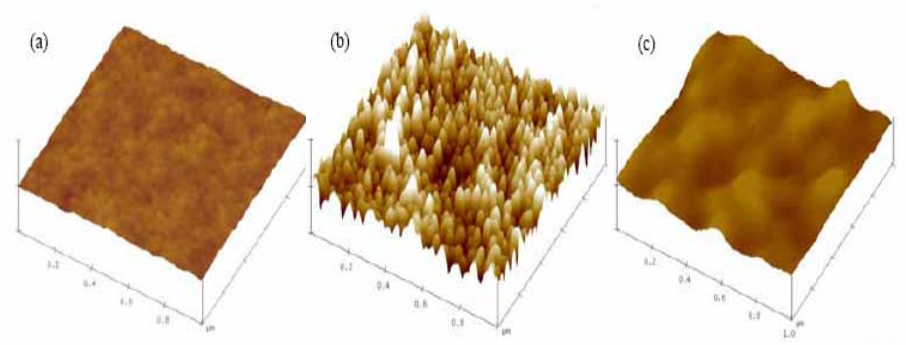

Fig 2. AFM scans of a) as deposited film surface, (b) surface after optimized $CF_4 + O_2$ etch, (c) optimized CHF_3 etch. Scan size is 1×1µm, vertical scale is 10 nm/div. RMS roughnesses are (a) 0.3 nm, (b) 3.3 nm, (c) 1.5 nm.

After resist removal with standard wet stripping, the waveguides were clad with a 15 µm thick film of UV cured inorganic polymer glass (RPO Pty Ltd, IPG™) which has a refractive index of 1.53 at 1550 nm. End facets were then prepared on the waveguides by hand cleaving the silicon substrate with a diamond scriber. The resulting waveguide chips were approximately 4 cm wide and 7.2 cm long. Figure 3 shows the end facet of a finished waveguide.

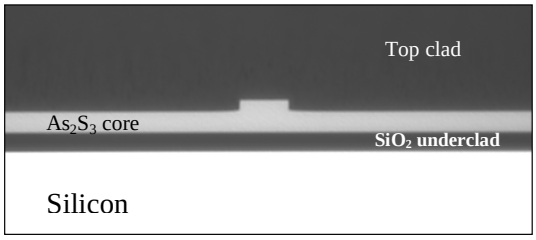

Fig. 3. Optical micrograph of cleaved finished waveguide in the 2.6 µm thick As_2S_3 film

3. Linear characterization

Insertion loss data was then gathered for all waveguides in the two snake designs and the 7.2 cm long straights between them. Fiber coupling was accomplished using lensed fibers with a 3.3 µm $1/e^2$ mode field diameter to suppress the Fabry-Perot cavity between the waveguide and fiber end faces. To avoid the Fabry-Perot effects within the waveguide chip itself, an external cavity tunable laser with linewidth broadened to greater than 7 times the minimum free spectral range of the waveguide chip was used as a source for the measurements at 1550 nm. Polarization dependent loss (PDL) data was gathered using a scanning polarisation controller.

Figure 4 shows insertion loss data for the 4 µm wide waveguides, including data for an additional 6 cm long straight waveguide chip from the wafer with 2.6 µm of As_2S_3. Five waveguides of each length were measured, and the measurement was repeated one week later using new lens coupling and zero offsets for the 1550nm data. The propagation loss at 1550 nm was estimated from a least squares linear fit to the data at 0.05dB/cm for the TE mode for the 2.6 µm film and 0.17 dB/cm for the 0.9 µm film. The very low losses were also obtained from a second measurement method that is not dependent on the repeatability of coupling between the fiber and the waveguide, namely the Fabry-Perot method. Here, by measuring the waveguide chip Fabry-Perot fringe contrast for the 7, 15, and 22cm waveguides within a single waveguide chip and then least squares fitting the facet reflectivity and propagation loss [14], we also obtained a value of 0.05dB/cm for the TE mode of waveguides in the 2.6 µm film. PDL averaged 0.35 dB for each of the 6, 7.1 and 15.5 cm long waveguides in the 2.6 µm film, including measurement system PDL of 0.15 dB and input coupling PDL of

#87277 - $15.00 USD Received 7 Sep 2007; revised 14 Oct 2007; accepted 15 Oct 2007; published 18 Oct 2007

0.12 dB. For reasons not yet clear to us, the PDL of the 22.5 cm waveguides rose to an average value of 2.4 dB (range 1.3 to 3.5dB). For the 0.9 μm film the PDL was at most 1 dB for all waveguide lengths. At 1310 nm the loss for the 2.6 μm film was slightly higher, 0.08±0.05 dB/cm, but the PDL was lower, 0.32 dB even for the 22.5 cm waveguides. These are the lowest optical losses ever reported for chalcogenide planar waveguides by up to a factor of four.

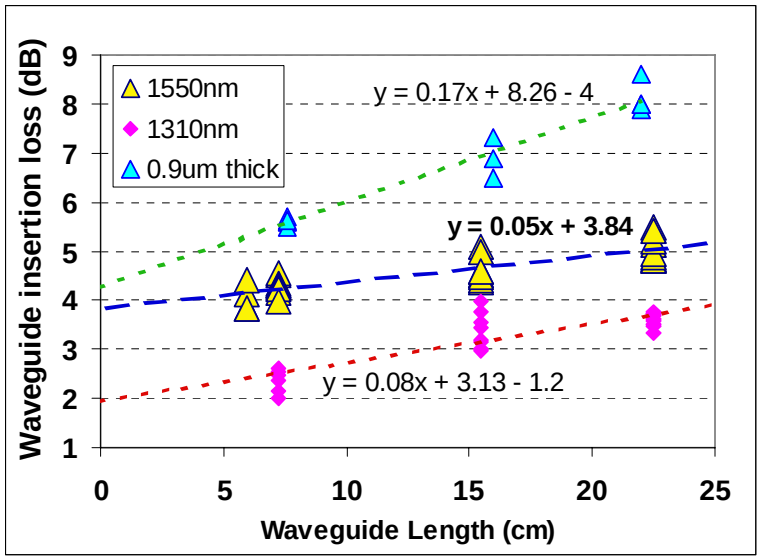

Fig. 4. Measured insertion loss for 2.5×4 μm and 0.9×4 μm waveguides. Data for the 1310 nm measurement and the 0.9 μm thick film have been offset for clarity.

The probable cause for the increase in loss at 1310 nm relative to 1550 nm is material absorption. Chalcogenide glasses display a characteristic exponentially-decaying absorption tail ($A_t e^{\hbar\omega/E_t}$) due to the presence of defects within their band gap [15]. Films contain larger numbers of defects compared with bulk glasses (as indicated by their different refractive index) and this results in losses in the 0.01-0.05 dB/cm range [16].

At present the reason for the higher loss for 0.9 μm thick films is not completely understood. However we observed that these waveguides supported the propagation of three modes and in the case of the 0.9 μm films this resulted in mode-beating at the output between the lowest order and first symmetric high order mode as the 1550 nm source was tuned. Compared with the thicker film, this mode is very close to cut-off and this could increase the losses to radiation for the higher order mode particularly at the bends.

Nevertheless these measured optical losses are low enough to allow fabrication of devices 20-60 cm long and this is up to ten times the largest value used in previous demonstrations of all-optical signal processing in chalcogenide planar waveguides [4]. The mode-field areas were calculated at 1550 nm using the full vector generic finite difference mode of the c2V Olympios software giving values of 7.1 μm^2 (7.6 μm^2) and 2.5 μm^2 (2.1 μm^2) for the TE (TM) modes in the 2.6 μm and 0.9 μm films respectively. The computed TE mode fields are shown in Fig. 5. For these waveguides the nonlinear parameters are ≈1700 /W/km and ≈4700 /W/km respectively. Assuming device lengths determined by 3-dB propagation loss, a nonlinear phase change of π can be obtained using pulse powers of ≈3 W in both instances in the absence of dispersive effects. A difference between these two waveguides is, however, their net dispersion. Olympios indicates the total dispersion of the 7.1 μm^2 waveguide was 433 ps^2/km for the TE mode at 1550 nm, and 406 ps^2/km for the TM mode. These figures are dominated by the intrinsic material dispersion of ≈470 ps^2/km. The dispersion is reduced to

#87277 - $15.00 USD Received 7 Sep 2007; revised 14 Oct 2007; accepted 15 Oct 2007; published 18 Oct 2007

352 ps^2/km and 110 ps^2/km for the TE and TM modes respectively in the 2.5 μm^2 waveguide due to competition between material and waveguide dispersion. For an optimized waveguide 2 μm wide in a 1 μm thick film and with 50% etch depth, the TM mode dispersion is predicted to drop to zero [17]. Thus the smaller mode area waveguides using the TM mode should enable efficient broadband phase-matched nonlinear processes such as wavelength conversion via four-wave mixing [17].

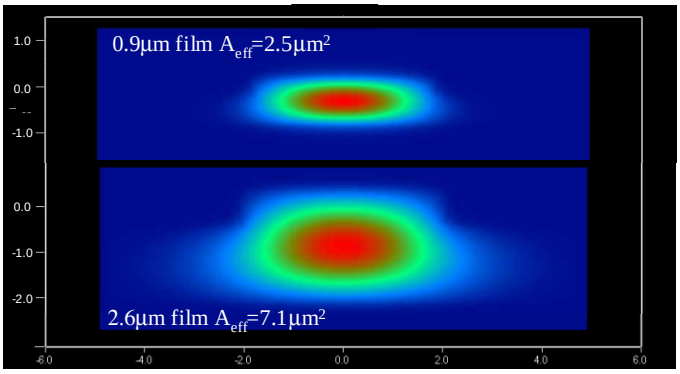

Fig. 5. Computed quasi-TE mode field of fabricated waveguides

An interesting point to note from the mode profiles is that there is little field concentration at the etched rib sidewalls, in contrast to typical nanowire devices [8]. This suggests even smaller mode areas may be obtainable whilst suffering only a moderate increase in losses from sidewall scattering.

Numerical modeling showed, for example, that for a 2 μm wide rib (undemanding lithography and the upper width limit of single mode operation of the waveguide) and film thicknesses down to 0.5 μm, the smallest mode area attainable for a 30-40% etch depth is 0.95 μm^2. For comparison, for the best nanowire design for this materials system (0.55×0.55 μm), the mode area is 0.35μm^2 but then field enhancement at the waveguide sidewalls is significant for the TE mode. For the rib design, and 1 μm film thickness (corresponding to a geometry where the total waveguide dispersion is expected to be ≈0) the mode area increases to 1.5 μm^2 but there is still little enhancement of the field at the etched sidewalls. Using the full vector two dimensional generic finite difference bent waveguide mode of Olympios (Bend2D) with >300 grid points in the in plane bend direction, we also established this design is single mode, capable of being bent with radii down to 1 mm with bend losses of below 0.01 dB/radian, and that both TE and TM modes propagate at 1550 nm with similar mode field dimensions.

4. Nonlinear pulse propagation and optical regeneration

To characterize the nonlinear properties of the waveguides we observed the nonlinear spectral broadening of pulses propagating through a 4 μm wide, 2.6 μm tall serpentine waveguide of length 22.5 cm. The setup, as shown in Fig. 6, was based on optical pulses of 1.2 ps duration generated from a passively mode-locked, figure-eight, fiber laser operating at a repetition rate of 4.0 MHz. The pulses were launched into the rib waveguide by direct butt-coupling via an intermediate section of high numerical aperture fiber (NA = 0.35) and index-matching oil to improve mode matching and remove fiber-waveguide Fabry-Perot effects, resulting in a total fiber-to-fiber insertion loss of 6.0 dB (≈1.1 dB due to propagation loss). A 1% fiber coupler and variable optical attenuator facilitated power control and a fiber based polarization controller was used to set the input to the lower loss TE polarization mode.

#87277 - $15.00 USD Received 7 Sep 2007; revised 14 Oct 2007; accepted 15 Oct 2007; published 18 Oct 2007

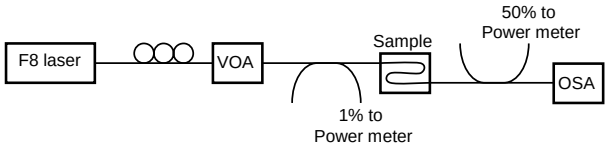

Fig. 6 Experimental setup for demonstration of spectral broadening. F8: figure eight fiber laser; VOA: variable optical attenuator; OSA: Optical spectrum analyzer.

Figure 7 (a) shows the experimentally observed self phase modulation (SPM) spectral broadening of the pulses resulting in 3 spectral lobes for an average power of 0.25 mW in fiber, corresponding to a calculated peak power of 23.7 W inside the waveguide. No nonlinear absorption (i.e. two photon absorption) was observed, in agreement with earlier measurements [4, 18]. Also plotted, in good agreement with the experimental data, are the results of simulations solving the nonlinear Schrödinger equation by the split-step Fourier method using parameters based on the experimental setup described above, with $n_2 = 2.92 \times 10^{-18}$ m^2W^{-1} [18]. The weak spectral oscillations on the pulses are due to the presence of strong normal dispersion within the waveguides which results in linear pulse chirp [19].

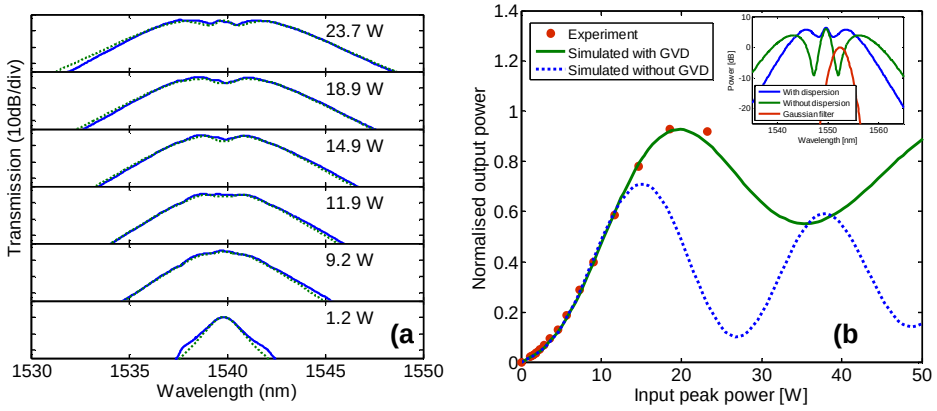

Fig. 7. (a) Spectral broadening of 1.2 ps pulses with peak power specified inside waveguide (experiment:solid and simulation:dashed). (b) Resulting regenerator power transfer function for a 2.8 nm spectrally offset Gaussian filter immediately after the waveguide. Inset shows filter spectrum and simulated broadening with and without dispersion at 23.7 W peak power.

The nonlinear spectral response of the waveguide makes it suitable for SPM based optical signal regeneration [11]. Such regenerators operate using a combination of SPM and a band-pass filter offset from the signal wavelength by more than the signal optical bandwidth so that at low intensities, the optical signal is blocked by the filter. At high intensities, (representing logical "1's") the pulses undergo sufficient spectral broadening so that a portion is transmitted through the pass band. At still higher intensities, the signal experiences significant broadening and the power within the transmission band pass saturates. The resulting "S-shaped" nonlinear power transfer curve is a hallmark of optical regenerators (for reshaping), and has the effect of reducing noise on both the signal "0's" and "1's".

Figure 7 (b) shows the resulting transfer function using the experimental and simulated spectra derived by adding a spectrally offset, Gaussian band-pass filter to the output of the waveguide. The 1.96 nm filter bandwidth was set to match the laser FWHM and offset to longer wavelengths by 2.8 nm (the inset overlays the band-pass filter spectrum onto the simulated spectra for a peak coupled power of 23.7 W). At lower peak powers the pulses are completely blocked by the offset filter, while high powers result in spectral slicing of the SPM induced spectral broadened pulses, generating a nonlinear transfer function. Also shown in Fig. 7 (b) is the simulated transfer function in the absence of normal dispersion. Comparing simulations shows that normal dispersion in the long serpentine waveguides improves the

#87277 - $15.00 USD Received 7 Sep 2007; revised 14 Oct 2007; accepted 15 Oct 2007; published 18 Oct 2007

saturation effect and reduces the modulation of the transfer function while only marginally increasing power requirements, enhancing the waveguide's potential regenerative performance [11, 20]. This is in contrast with our earlier report based on a shorter 5 cm waveguide where the effects of dispersion were negligible [18]. In assessing the serpentine chalcogenide glass waveguides for SPM based optical regeneration we find that both the large nonlinearity and high dispersion, which result in weak SPM spectral oscillations, contribute to device performance.

5. Summary

In conclusion, we have demonstrated As_2S_3 waveguides up to 22.5 cm long with losses down to 0.05 dB/cm at 1550 nm, the lowest ever reported by a factor of 4×. It appears there is a realistic prospect of achieving similar losses in waveguides with mode areas as low as 1 μm^2. Furthermore using chalcogenide glasses with higher nonlinearity (e.g. ×4 is possible using Ge-As-Se glasses, [1]), a peak power for all-optical signal processing below 1 W will be achieved. We show the suitability of these waveguides for all-optical signal processing by demonstrating spectral broadening of picosecond duration pulses, in excellent agreement with theory. Furthermore, simulations show that the group velocity dispersion of these waveguides results in a near optimal nonlinear transfer function for all-optical signal regeneration of high data rate signals.

Acknowledgement

The support of the Australian Research Council through its Centres of Excellence, Federation Fellow and Discovery grant programs is gratefully acknowledged.

#87277 - $15.00 USD Received 7 Sep 2007; revised 14 Oct 2007; accepted 15 Oct 2007; published 18 Oct 2007